



Similarity of climate control on base flow and perennial stream density in the Budyko framework

D. Wang and L. Wu

Department of Civil, Environmental, and Construction Engineering, University of Central Florida, Orlando, FL 32816, USA

Correspondence to: D. Wang (dingbao.wang@ucf.edu)

Received: 31 May 2012 – Published in Hydrol. Earth Syst. Sci. Discuss.: 14 June 2012

Revised: 14 December 2012 – Accepted: 21 December 2012 – Published: 25 January 2013

Abstract. Connection between perennial stream and base flow at the mean annual scale exists since one of the hydrologic functions of perennial stream is to deliver runoff even in low flow seasons. The partitioning of precipitation into runoff and evaporation at the mean annual scale, on the first order, is captured by the ratio of potential evaporation to precipitation (E_p/P called climate aridity index) based on Budyko hypothesis. Perennial stream density (D_p), which is obtained from the high resolution National Hydrography Dataset, for 185 watersheds declines monotonically with climate aridity index, and an inversely proportional function is proposed to model the relationship between D_p and E_p/P . The monotonic trend of perennial stream density reconciles with the Abrahams curve since perennial stream density is only a small portion of the total drainage density. The correlation coefficient between the ratio of base flow to precipitation (Q_b/P), which follows a complementary Budyko type curve and perennial stream density is found to be 0.74. The similarity between Q_b/P and D_p reveals the co-evolution between water balance and perennial stream network.

density and PE index. Madduma Bandara (1974) extended the samples to cover watersheds in the humid Sri Lanka and a positive correlation was found between drainage density and PE index. Therefore, drainage density decreases but then increases from arid to humid regions (Abrahams, 1984), and this trend has been explained by the vegetation imparted to the soil (e.g., Moglen et al., 1998) and demonstrated in landscape evolution models (e.g., Perron et al., 2007; Collins and Bras, 2010).

Functional patterns offer an insight on the mechanisms and processes driving the observed natural structure (Sivapalan et al., 2011). The functional approach may provide answers as to why streams and their associated densities organize the way they do. The basic functions of a watershed include partition of collected water into different flowpaths, storage of water in different parts of the watershed, and release of water from the watershed (Wagener et al., 2007). Delivering the runoff generated in a watershed is one of the major hydrologic functions of stream network. On this basis, stream densities can be related to runoff in a watershed. Berger and Entekhabi (2001) and Sankarasubramanian and Vogel (2002b) studied the correlations between runoff coefficient and physiographic and climate variables (i.e., climate aridity index, drainage density, median slope, relief ratio, and infiltration capacity), and found that the ratio of potential evaporation and precipitation (E_p/P), which is called climate aridity index, explained most of variability of observed runoff coefficient which is also correlated with drainage density. The linkage between drainage density and frequency regimes of peak flows has also been discussed in the literature (Merz and Blöschl, 2008; Pallard et al., 2009).

In a watershed, the flowing stream network expands as a response to rainfall events and contracts during drought

1 Introduction

Total drainage density, defined as the total length of channels per unit area (Horton, 1932, 1945), is known to vary with climate and vegetation (Melton, 1957), soil and rock properties (Carlston, 1963; Kelton and Wells, 1989), and topography (Montgomery and Dietrich, 1988). Melton (1957) explored the dependence of drainage density on the Thornthwaite's (1931) precipitation effectiveness index (i.e., PE index) which is a measure of the availability of moisture to vegetation, and found a negative correlation between drainage

periods (Blyth and Rodda, 1973; Gregory, 1976; Day, 1978). From the perspective of flow duration, streams are categorized into perennial, intermittent, and ephemeral streams. Perennial stream, i.e., the basic stream network flowing for much of the year, is governed by groundwater flow and therefore depends upon mean annual precipitation as modified by watershed characteristics; temporal streams, i.e., intermittent or ephemeral, occur once or more each year and are responses to seasonal climate and individual rainfall events (Gregory, 1976). De Wit and Stankiewicz (2006) studied the relation between perennial stream density (D_P), which is the ratio between total perennial stream length and drainage area, and mean annual precipitation in Africa. They found that D_P is close to zero when precipitation is less than 400 mm yr^{-1} ; from 400 mm yr^{-1} to 1000 mm yr^{-1} , D_P increases with precipitation and then decreases when precipitation is larger than 1000 mm yr^{-1} .

However, runoff at the mean annual scale is not only controlled by water supply but also energy supply. Budyko (1958) postulated that mean annual evaporation from a watershed could be determined, to first order, from precipitation and potential evaporation. Based on worldwide data on a large number of watersheds, Budyko (1974) demonstrated that the partitioning of precipitation into runoff and evaporation is primarily controlled by climate aridity index. Perennial stream density may be dependent on both mean annual precipitation and potential evaporation similar to mean annual runoff, particularly base flow.

Interactions between climate, soil, vegetation, and topography contribute to the generation of observed patterns in natural watersheds, and the patterns contain valuable information about the way they function (Sivapalan, 2005). The dependence of perennial stream density on mean climate deserves further investigation for assessing potential climate change impact on water supply availability. The purpose of this research is to explore the dependences of both base flow and perennial stream density on climate aridity index and the co-evolution of water balance and perennial streams. The finding on perennial stream is compared with the Abrahams curve on total drainage density (Abrahams, 1984). Furthermore, the linkage between runoff from mean annual to event scales and perennial, intermittent and ephemeral stream densities is discussed.

2 Methodology

2.1 Data sources

The Model Parameter Estimation Experiment (MOPEX) watersheds are chosen as case study watersheds because precipitation, potential evaporation and runoff datasets are available. The MOPEX dataset is described by Duan et al. (2006). This dataset includes daily values of areal precipitation, climatologic potential evaporation, and streamflow with an

adequate number of precipitation gauges. Several recent studies have been based on the MOPEX watersheds (e.g., Sivapalan et al., 2011; Harman et al., 2011; Wang and Hejazi, 2011; Wang and Alimohammadi, 2012). Due to the missing data in both MOPEX and perennial stream datasets for some watersheds, 185 watersheds are selected in this study. Over the study watersheds, the climate aridity index ranges from 0.26 (humid) to 5.50 (arid). The minimum mean annual precipitation is 277 mm, and the maximum mean annual precipitation is 2771 mm.

Perennial streams are obtained from the National Hydrography Dataset (NHD) which is a comprehensive set of digital spatial data that encodes information about naturally occurring and constructed streamlines (<http://nhd.usgs.gov/>). The map scale of the high-resolution NHD is 1 : 24 000. All flow lines have been classified as perennial, intermittent, ephemeral streams, and others. The stream classification is based on digitizing the “blue line mapping” and stream symbolization on US Geological Survey (USGS) 7.5 min quadrangle topographic maps. The blue-line mapping and perennial and ephemeral or intermittent classifications on topographic maps used in the NHD are based on aerial photo interpretation and have been extensively verified by field reconnaissance by the USGS at the time the map was compiled or revised (Simley, 2003). Errors may occur in the process of digitally capturing the topographic map information and incorporating it into the NHD flow lines. Climate change, landscape change, human engineering and other variables present opportunities for improvement (Simley, 2007).

In the high-resolution NHD, each feature has its unit code which is five-digit integer value comprised of the feature type and the combinations of characteristics and values. In the dataset, streamlines are classified into perennial (46 006), intermittent (46 003), ephemeral streams (46 007), and others. Some perennial streams with human interferences are classified as artificial path (55 800), connector (33 400), or others. Therefore, these types of flow lines located in main channels should be accounted for in perennial streams when the total perennial stream length is computed. It should be noted that the value of total stream length, particularly for temporal (i.e., intermittent and ephemeral) streams, depends on the resolution of the map from which the streams were obtained (Montgomery and Dietrich, 1988). The temporal streams in the NHD are usually underestimated since the small order headwater streams are usually not accounted for due to the limited spatial resolution of the topographic map. However, this research is focused on perennial stream which is much more reliable than temporal streams in the NHD dataset.

2.2 Budyko hypothesis and complementary Budyko-type curves

The pattern of mean annual evaporation can be described by the Budyko curve, which shows a predictable relationship between annual water balance and the climatic drivers

of precipitation and potential evaporation (Budyko, 1974). Based on datasets from a large number of watersheds, Budyko (1974) proposed a relationship between mean annual evaporation ratio (E/P) and mean annual climate aridity index (E_p/P):

$$\frac{E}{P} = \sqrt{\frac{E_p}{P} \left[1 - \exp\left(-\frac{E_p}{P}\right) \right] \tanh\left(\frac{1}{E_p/P}\right)}, \quad (1)$$

where E is the mean annual evaporation. Gerrits et al. (2009) provided a theoretical backing for the empirical Budyko curve by using a simple evaporation model and rainfall characteristics. As shown in Fig. 1, evaporation ratio, which is captured by the Budyko curve, increases from humid to arid regions. The slope of the Budyko curve is steep in energy-limited regions (i.e., $E_p/P < 1$), and becomes flat in water-limited regions ($E_p/P > 1$). Other functional forms of Budyko-type curves have been developed for assessing long-term water balance (e.g., Turc, 1954; Pike, 1964; Fu, 1981; Zhang et al., 2001; Sankarasubramanian and Vogel, 2002a; Yang et al., 2008). One of the Budyko-type functions is the Turc–Pike equation:

$$\frac{E}{P} = \left[1 + \left(\frac{E_p}{P}\right)^{-v} \right]^{-1/v}, \quad (2)$$

where v is the parameter that represents the effects of other factors, such as vegetation, soil, and topography, on the partitioning of precipitation.

The mean annual precipitation, potential evaporation, and runoff (Q) for the study watersheds are computed based on the available data of daily precipitation, runoff, and climatic potential evaporation. Climate data is available during 1948–2003. Even though the general findings on climate control on perennial stream density are not affected by the selection of period for hydro-climatic data, the mean annual E/P and E_p/P during 1948–1970 are used considering the time period when the perennial stream data was constructed. As shown in Fig. 1, the observed mean annual evaporation ratio for the study watersheds (i.e., blue circle) is along the Budyko curve (i.e., red line). The scatter of the data points in Fig. 1 is caused by data uncertainty and other controlling factors such as climate seasonality, vegetation, soil, and topography (Milly, 1994; Zhang et al., 2001; Donohue et al., 2007; Yang et al., 2007; Yokoo et al., 2008; Zhang et al., 2008). At the mean annual scale, the steady-state condition can be assumed for water balance. Runoff coefficient (Q/P) can be estimated by the complementary Budyko-type curve, i.e., $Q/P = 1 - E/P$.

Similar to runoff coefficient, base flow coefficient, which is defined as the ratio of mean annual base flow (Q_b) to precipitation, is also mainly controlled by climate aridity index. Mean annual base flow is computed by conducting base flow separation using a one-parameter low-pass filter method (Lyne and Hollick, 1979). For consistency, the value of the

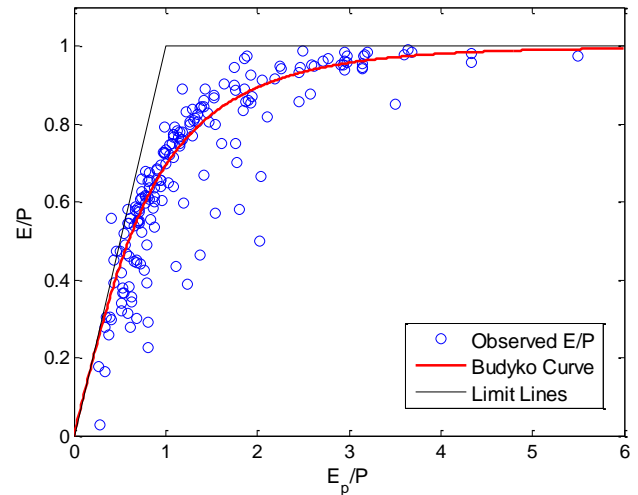


Fig. 1. Comparison of observed evaporation ratio (E/P) with estimates based on Budyko curve at 185 MOPEX catchments.

filter parameter is set to 0.925 for all the watersheds (Sivapalan et al., 2011). Base flow coefficients of the case study watersheds are plotted in Fig. 2 as a function of climate aridity index. A complementary Turc–Pike curve is fitted to the observed data points:

$$\frac{Q_b}{P} = 1 - \left[1 + \left(\frac{E_p}{P}\right)^{-3.3} \right]^{-1/3.3}. \quad (3)$$

The estimated value for the parameter v is 3.3 for the data points in Fig. 2.

2.3 Perennial stream density as a function of climate aridity index

The differentiation between perennial and temporal streams is not quantitatively definite, and subject to a variety of definitions adopted by regulation agencies and academics with a need to classify streamflow durations. Therefore, definitions of perennial and temporal streams vary widely among regulatory agencies. For example, a perennial stream is defined as a river channel that has continuous flow on the stream bed all year round during years of normal rainfall (Meinzer, 1923). Perennial streams are defined as having 7-day, 10-yr low flows greater than zero by Hunrichs (1983). During unusually dry years, a normally perennial stream may cease flowing, becoming intermittent for days, weeks, or months depending on severity of the drought (Ivkovic, 2009). Perennial stream in the NHD dataset is defined as “stream contains water throughout the year, except for infrequent periods of severe drought” (Simley, 2006).

Generally, perennial stream density (D_p) is higher in humid regions than that in arid regions. Perennial stream networks are mainly controlled by mean climate as well as other factors such as lithology and topography. The hydrologic

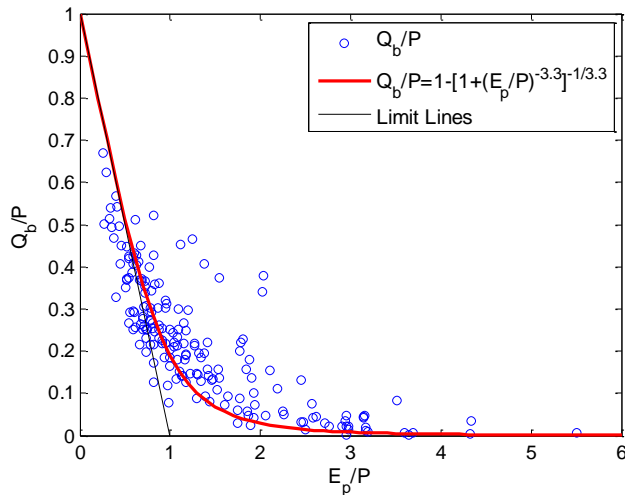


Fig. 2. Q_b/P versus E_p/P , and the fitted complementary Turc-Pike curve.

function of perennial streams is to deliver runoff, particularly during low flow seasons when base flow is dominant. As discussed above, the pattern of Q_b/P can be captured by the complementary Budyko-type curve shown in Eq. (3). In this paper, the correlation between D_p and Q_b/P is evaluated.

3 Results

Perennial stream length and density are computed for each watershed studied based on the NHD dataset. Figure 3 shows the perennial and temporal streams for four selected watersheds with different climate aridity index. The climate aridity index and perennial stream density for the Snoqualmie River watershed located in the State of Washington is 0.29 and 1.60 km km^{-2} , respectively (Fig. 3a). However, in the arid region of New Mexico ($E_p/P = 5.50$), the perennial stream density for the Arroyo Chico watershed is only 0.067 km km^{-2} (Fig. 3d). Figure 3b and c show the perennial stream network at the other two watersheds with climate aridity index of 0.70 and 1.77, respectively. Perennial stream densities decrease from energy-limited to water-limited regions. The spatial distribution of perennial stream densities for all the case study watersheds is shown in Fig. 4. As we can see, perennial stream densities are higher in the eastern US and relatively low in the Great Plains. The minimum perennial stream density is 0 km km^{-2} and the maximum perennial stream density is 1.60 km km^{-2} over the 185 watersheds. When the drainage area is not large enough to sustain perennial streams in arid regions, perennial stream density can be zero. There are two watersheds with zero perennial stream density: Conchas Creek in New Mexico with a drainage area of 1230 km^2 , and Los Gatos Creek above Nunez Canyon in California with a drainage area of 247 km^2 .

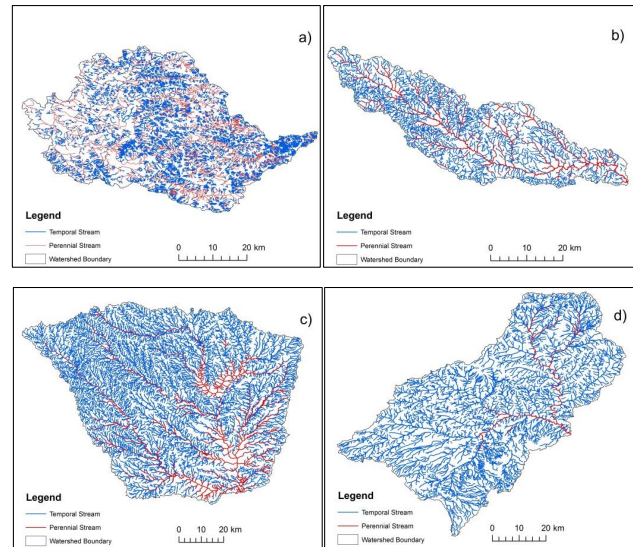


Fig. 3. Temporal stream and perennial stream: (a) Snoqualmie River watershed, Washington with USGS gage 12149000, $E_p/P = 0.29$, $D_p = 1.60 \text{ km}^{-1}$; (b) Red Creek watershed, Mississippi with USGS gage 02479300, $E_p/P = 0.70$, $D_p = 0.48 \text{ km}^{-1}$; (c) Elm Fork Trinity River watershed, Texas with USGS gage 08055500, $E_p/P = 1.77$, $D_p = 0.27 \text{ km}^{-1}$; (d) Arroyo Chico watershed, New Mexico with USGS gage 08340500, $E_p/P = 5.50$, $D_p = 0.067 \text{ km}^{-1}$.

The perennial stream densities obtained from the NHD dataset are compared with the reported ones in the literature. De Wit and Stankiewicz (2006) reported the perennial stream densities in Africa and the values vary from 0 to 0.14 km km^{-2} . In a small peatland headwater catchment in United Kingdom, the perennial stream density is 1.41 km km^{-2} when water tables fall below 180 mm, but the total drainage density is 29.98 km km^{-2} when the stream network is fully expanded (Goulsbra et al., 2012). This implicates that active streams are stabilized when the water table is below 180 mm. The perennial stream density in the Turnhole Bend Groundwater Basin in Kentucky is reported in values ranging from 0.24 km km^{-2} to 1.13 km km^{-2} . Johnston and Shmagin (2008) reported that the average perennial stream density of several watersheds located in the Great Lakes is 0.42 km km^{-2} . Perennial stream density in the Northern Rockies ecoregion is relatively high and the values reported range from 0.9 km km^{-2} to 1.2 km km^{-2} (McIntosh et al., 1995). Wigington et al. (2005) reported that perennial stream density of agricultural watersheds in western Oregon varies from 0.24 km km^{-2} to 0.66 km km^{-2} even though the total stream density varies from 2.90 km km^{-2} to 8.00 km km^{-2} . The perennial stream density for the four case study watersheds located in western Oregon are 0.1 km km^{-2} (USGS gage 14308000), 0.26 km km^{-2} (USGS gage 11497500), 0.29 km km^{-2} (USGS gage 14080500), and 0.67 km km^{-2} (USGS gage 11532500) as shown in Fig. 4. The magnitude of

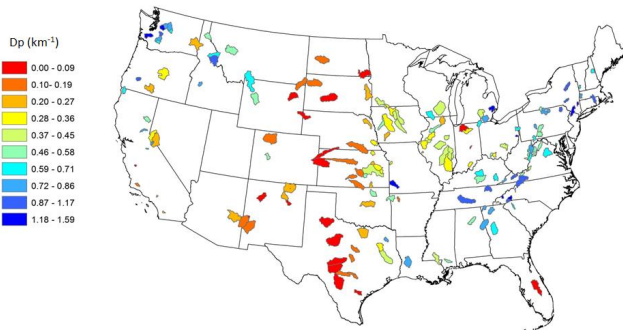


Fig. 4. Spatial distribution of perennial stream densities for the case study watersheds.

perennial stream density computed based on the NHD dataset is consistent with these reported values in the literature.

To explore the climate control on perennial streams, perennial stream densities of all the study watersheds are plotted as a function of climate aridity index (Fig. 5). The blue circles represent the NHD-based perennial stream density which monotonically decreases with climate aridity index. The narrow-banded data cloud shows the strong dependence of perennial stream density on E_p/P . De Wit and Stankiewicz (2006) studied the mean annual precipitation control on perennial stream density in Africa, and proposed a non-monotonic relationship. Annual precipitation has usually been the main focus in studies of climate control on drainage density (e.g., Abrahams and Ponczynski, 1984). To include the effect of energy, PE index proposed by Thornthwaite (1931) contains both precipitation and actual evaporation which is implicitly related to temperature (Moglen et al., 1998). However, from the perspective of water balance, the hydrologic basis of the PE index is not as strong as that of the climate aridity index proposed by Budyko (1958). Gregory (1976) compared the pattern of total drainage density as a function of climate aridity index, but no explicit pattern was discovered. The reason is that the dependence of temporal streams on mean climate is not as strong as perennial streams. As we expect, a monotonic trend is identified for perennial stream density as a function of climate aridity index in this study. An inversely proportional function is proposed to fit the data points in Fig. 5:

$$D_p = \frac{k}{E_p/P}, \tag{4}$$

where the coefficient k represents the perennial stream density for watersheds with balanced water and energy supply ($E_p/P = 1$), and the value of k is 0.44 km km^{-2} based on the fitted curve.

Since perennial stream is defined as the active stream during drought periods when base flow dominates the streamflow, perennial stream density may be correlated with base flow coefficient. As shown in Fig. 6, the correlation between perennial stream density and base flow coefficient is indeed

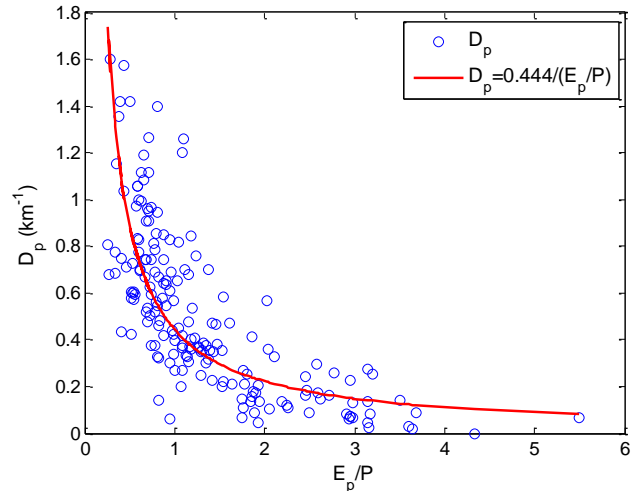


Fig. 5. NHD-based perennial stream density, D_p (km^{-1}), and the fitted line are plotted as a function of climate aridity index (E_p/P).

strong, and the correlation coefficient between them is 0.74. Furthermore, since the climate aridity index is the first order control on both Q_b/P (Fig. 2) and D_p (Fig. 5), similarity exists between the base flow coefficient and the perennial stream density in the dependence on mean annual climate aridity index.

4 Discussions

4.1 Perennial, intermittent, ephemeral, and total stream densities

The Abrahams curve (Fig. 7) represents the dependence of total drainage density (D_d) on PE index which is computed by

$$PE = 10 \sum_{m=1}^{12} \frac{P_m}{E_{p_m}}, \tag{5}$$

where P_m and E_{p_m} are mean monthly precipitation and potential evaporation, respectively (Thornthwaite, 1931). As shown in Fig. 7, D_d decreases and then increases with PE index (Abrahams, 1984). The relationship between PE index and E_p/P for the case study watersheds is shown in Fig. 8. Higher PE index is corresponding to lower E_p/P , and the correlation coefficient between PE and E_p/P is -0.73 .

To explore the contribution of perennial stream density to total drainage density reported by Abrahams (1984), perennial stream densities for the case study watersheds are added to the Abrahams curve in Fig. 7. As we can see, perennial stream density increases with PE index. Perennial stream density is only a small portion of the total drainage density, and the trend of intermittent and ephemeral streams dominates that of total drainage density. However, perennial stream density contributes to the increasing trend of total

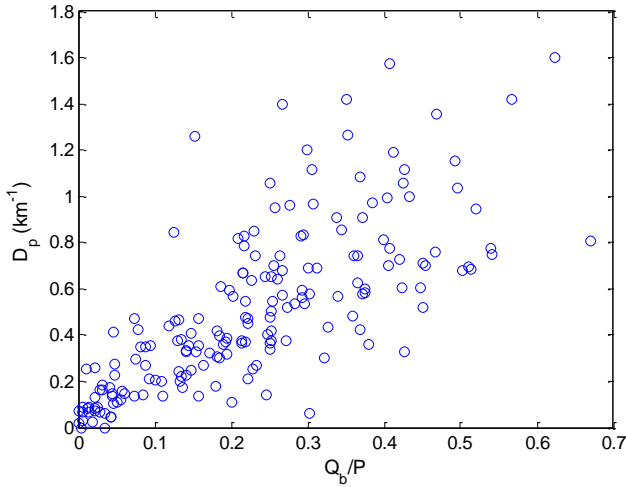


Fig. 6. The correlation coefficient between perennial stream density (D_p) and base flow coefficient (Q_b/P) is 0.74.

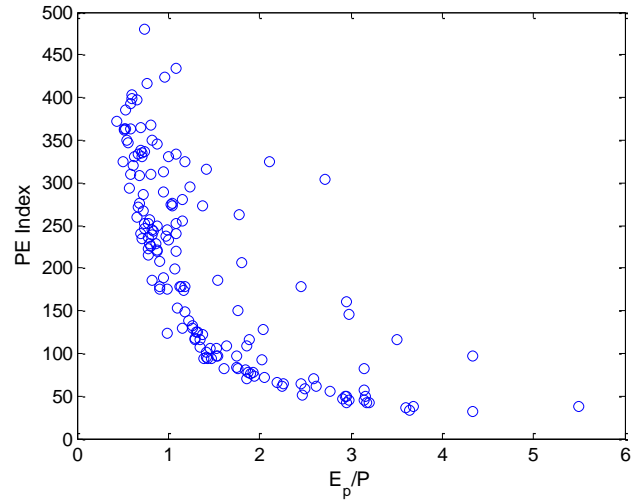


Fig. 8. The correlation between PE index and climate aridity index (E_p/P) for the 160 study watersheds with PE index less than 500.

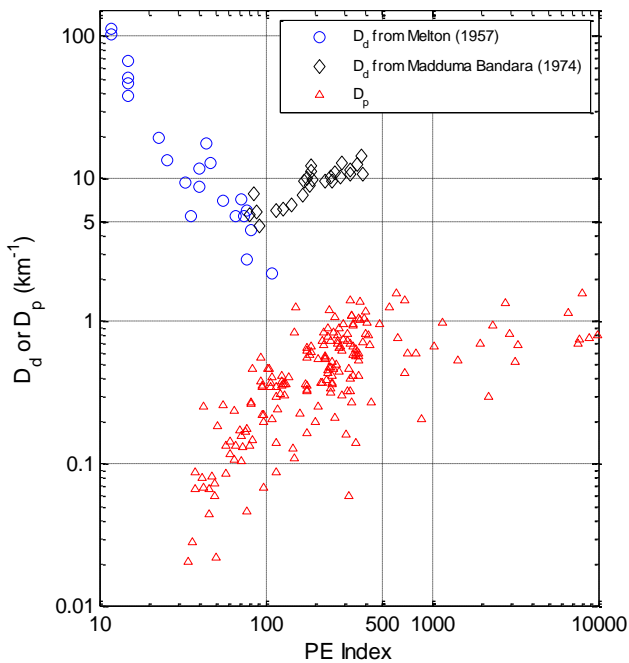


Fig. 7. Total drainage density (Abrahams, 1984) and perennial stream density as a function of PE index.

drainage density when PE index is higher than 100. Therefore, the findings on perennial stream density in this study do not contradict the Abrahams curve when PE index is below 100.

The observed non-monotonic trend of total drainage density as a function of PE index has been explained by the tradeoff between runoff erosion and resistance by vegetation (Abrahams, 1984). In the Abrahams curve shown in Fig. 7, the declining trend of D_d is due to the increase of vegetation resistance but the increasing trend is due to the increase

of runoff erosion. As an alternative, the non-monotonic trend may be explained by the runoff generation at different temporal scales (Fig. 9). Definitions of perennial, intermittent and ephemeral streams are based on the streamflow duration in each river segment. Perennial stream is defined as the active stream even in drought periods. Therefore, mean climate control on perennial stream density and base flow coefficient is similar as discussed earlier. Intermittent stream is defined as seasonally active one, and intermittent stream density (D_i) may be related to the seasonal water balance. Ephemeral stream density (D_e) is corresponding to high flows corresponding to extreme rainfall events. To fully reveal the co-evolution of total stream density and water balance at various temporal scales, the patterns of D_i and D_e as a function of E_p/P need to be further quantified in the future when accurate data is available.

4.2 Normalized perennial stream density

In order to compare the similarity of climate control on base flow and perennial stream in the Budyko framework, perennial stream density needs to be converted into a dimensionless number like the base flow coefficient. The perennial stream density in each watershed is then normalized by the maximum potential perennial stream density denoted as D_p^* . The normalized perennial stream density, D_p/D_p^* , can be plotted in the Budyko framework and compared with the complementary Budyko-type curve. However, it is a challenge to identify the maximum potential perennial stream density in each watershed. In this study, the total temporal and perennial stream density obtained from the NHD dataset is used for D_p^* . It should be noted that the NHD dataset is based on topographic maps equivalent to 30 m DEM. Total drainage densities are smaller than the values in Fig. 7, and

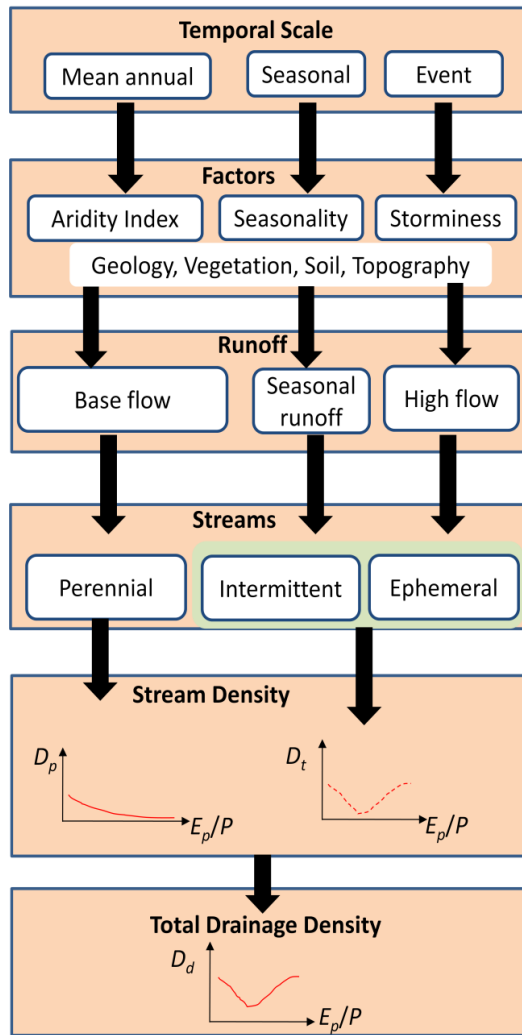


Fig. 9. Perennial, intermittent and ephemeral streams and runoff generation from mean annual to seasonal and to event scales. The trend of D_t , which is the intermittent and ephemeral stream density, as a function of E_p/P is hypothetical.

there is no obvious pattern in the relationship between the total density of perennial and temporal streams from the NHD and PE index or E_p/P .

The normalized perennial stream density is plotted in Fig. 10 as a function of E_p/P . The red line in Fig. 10 is the fitted Turc–Pike equation for base flow coefficient shown in Fig. 2. Data points for D_p/D_p^* is a little bit above the red line. Considering the uncertainty of datasets and potential underestimation of D_p^* , the similarity between D_p/D_p^* and Q_b/P as a function of E_p/P is promising based on the case study watersheds. The limit lines for base flow coefficient are represented by black lines in Fig. 10. Due to the uncertainty in the hydro-climatic data, several data points (E/P) are located above the limit line, i.e., the 1 : 1 line shown in Fig. 1. However, more data points for D_p/D_p^* are located

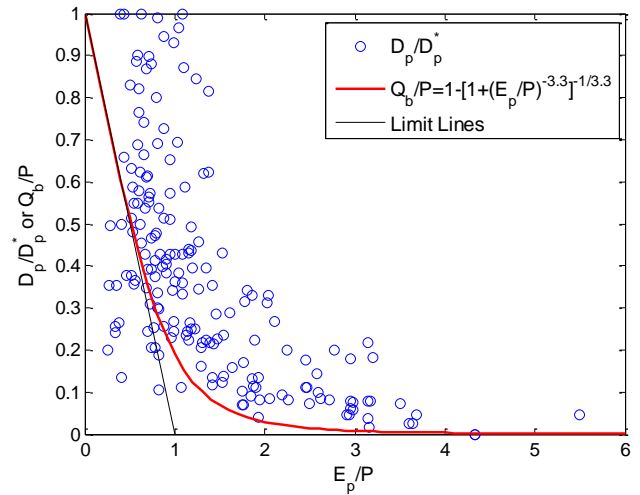


Fig. 10. D_p/D_p^* versus E_p/P and the fitted complementary Turc–Pike curve for Q_b/P versus E_p/P .

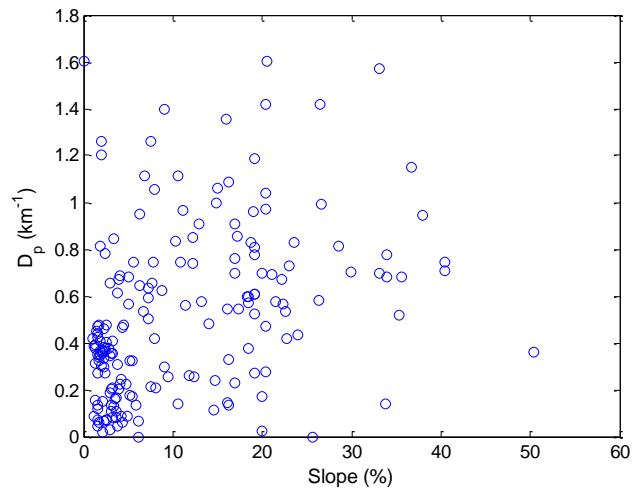


Fig. 11. Perennial stream density versus slope (%) for the case study watersheds.

below the limit line in Fig. 10. Besides uncertainty of perennial stream data in the NHD dataset, the value of D_p^* can also affect the position of these points. Long-term climate may not be the main controls in some special watersheds and perennial stream density is high due to geology and lithology. The data points in Fig. 10 may be not necessarily above the limit line, i.e., $D_p/D_p^* > 1 - E_p/P$. Even though the similarity exists in the base flow coefficient and perennial stream density dependence on long-term mean climate, the controls of other factors on water balance and perennial stream may be different.

4.3 Impact of slope on perennial stream density

Besides mean climate, the topographic control on perennial stream density is investigated here. The average slope for each watershed is computed by using the 90-m DEM SRTM data for North America downloaded from http://dds.cr.usgs.gov/srtm/version2_1/SRTM3/. Figure 11 shows the relationship between perennial stream density and slope by percentage. Generally, high perennial stream density is associated with higher slope, but the dependence is not strong as climate aridity index shown in Fig. 5. It should be noted that slope is also related to climate aridity index in certain levels. Therefore, mean annual climate is the first order control on perennial stream density like rainfall partitioning, but other factors such as slope may be the second order control.

4.4 Application of the relationship between perennial stream density and climate aridity index

One of the purposes for this research is to develop a simple model to predict perennial stream density. For example, De Wit and Stankiewicz (2006) applied the step-wise linear relationship between mean annual precipitation and perennial stream density to assess the climate change impact on perennial stream density in Africa. In this paper, an inversely proportional function is developed to predict perennial stream densities based on climate aridity index. The scatters in Fig. 5 reflect the impact of other factors on perennial stream density. Empirical relationships between the values of parameter k and the other factors can be constructed so that perennial stream density can be predicted more accurately. In global hydrological models, an estimate of the perennial stream density for each grid cell (e.g., $0.5^\circ \times 0.5^\circ$) is needed in order to model the local groundwater level and the groundwater discharge (Van Beek and Bierkens, 2008; Wu et al., 2011). The findings from this research will provide a framework to modeling perennial stream density for macroscale hydrological model development.

5 Conclusions

The observed pattern of perennial stream density can be explained by the hydrologic functions of perennial streams. Climate aridity index is the first order control on perennial stream density, and an inversely proportional function is used to model the dependence of perennial stream density on the climate aridity index. Therefore, the perennial stream density is one component of co-evolution of climate, vegetation, soil, and landscape at the mean annual scale. Furthermore, perennial stream density is strongly correlated with the base flow coefficient which is the ratio of mean annual base flow to precipitation. Similarity may exist between the dependences of normalized perennial stream density and the base flow coefficient on climate aridity index and the climate control is quantified by complementary Budyko-type curves.

In this study, we only focus on the first order control (i.e., mean climate) on perennial stream density. The scatters of the normalized perennial stream density in the Budyko framework are due to other factors such as vegetation type and coverage, soil, topography, geology, etc. Future efforts can investigate the impact of these factors on the perennial stream density from the perspective of hydrologic functions in the Budyko framework. The maximum perennial stream density, which is the normalization factor, is estimated based on the NHD dataset. The maximum perennial stream density for individual watershed is open for further investigation. To fully reveal the co-evolution between water balance and total drainage density, intermittent and ephemeral stream densities need to be quantified, respectively.

Acknowledgements. Partial financial support was provided by the Florida Sea Grant NA10OAR4170079 and NOAA grant NA10NOS4780146. The authors are grateful to the insightful comments, which lead to improvement of this manuscript, by Murugesu Sivapalan, Hubert H. G. Savenije, Kyungrock Paik, Huan Wu, one anonymous reviewer and the Associate Editor Ciaran Harman.

Edited by: C. Harman

References

- Abrahams, A. D.: Channel Networks: A Geomorphological Perspective, *Water Resour. Res.*, 20, 161–188, doi:10.1029/WR020i002p00161, 1984.
- Abrahams, A. D. and Ponczynski, J. J.: Drainage density in relation to precipitation intensity in the USA, *J. Hydrol.*, 75, 383–388, 1984.
- Berger, K. P. and Entekhabi, D.: Basin hydrologic response relations to distributed physiographic descriptors and climate, *J. Hydrol.*, 47, 169–182, 2001.
- Blyth, K. and Rodda, J. C.: A stream length study, *Water Resour. Res.*, 9, 1454–1461, doi:10.1029/WR009i005p01454, 1973.
- Budyko, M. I.: *The Heat Balance of the Earth's Surface*, translated from Russian by: Stepanova, N. A., 259 pp., US Dep. of Commer., Washington DC, 1958.
- Budyko, M. I.: *Climate and Life*, 508 pp., Academic Press, New York, 1974.
- Carlston, C. W.: *Drainage Density and Stream Flow: US Geological Survey Professional Paper No. 422-C*, 1–8, 1963.
- Collins, D. B. G. and Bras, R. L.: Climatic and ecological controls of equilibrium drainage density, relief, and channel concavity in dry lands, *Water Resour. Res.*, 46, W04508, doi:10.1029/2009WR008615, 2010.
- Day, D. G.: Drainage density changes during rainfall, *Earth Surf. Processes*, 3, 319–326, 1978.
- De Wit, M. and Stankiewicz, J.: Changes in surface water supply across Africa with predicted climate change, *Science*, 311, 1917–21, 2006.

- Donohue, R. J., Roderick, M. L., and McVicar, T. R.: On the importance of including vegetation dynamics in Budyko's hydrological model, *Hydrol. Earth Syst. Sci.*, 11, 983–995, doi:10.5194/hess-11-983-2007, 2007.
- Duan, Q., Schaake, J., Andréassian, V., Franks, S., Goteti, G., Gupta, H. V., Gusev, Y. M., Habets, F., Hall, A., Hay, L., Hogue, T., Huang, M., Leavesley, G., Liang, X., Nasonova, O. N., Noilhan, J., Oudin, L., Sorooshian, S., Wagener, T., and Wood, E. F.: The Model Parameter Estimation Experiment (MOPEX): An overview of science strategy and major results from the second and third workshops, *J. Hydrol.*, 320, 3–17, 2006.
- Fu, B. P.: On the calculation of the evaporation from land surface, *Scientia Atmospherica Sinica*, 5, 23–31, 1981.
- Gerrits, A. M. J., Savenije, H. H. G., Veling, E. J. M., and Pfister, L.: Analytical derivation of the Budyko curve based on rainfall characteristics and a simple evaporation model, *Water Resour. Res.*, 45, W04403, doi:10.1029/2008WR007308, 2009.
- Goulsbra, C., Evans, M., and Lindsay, J.: Temporary streams in a peatland catchment: the pattern and timing of stream network expansion and contraction and controls on these, *Geophys. Res. Abstr.*, 14, EGU2012-11014-1, 2012.
- Gregory, K. J.: Drainage networks and climate, in: *Geomorphology and Climate*, edited by: Derbyshire, E., 289–315, John Wiley, New York, 1976.
- Harman, C. J., Troch, P. A., and Sivapalan, M.: Functional model of water balance variability at the catchment scale: 2. Elasticity of fast and slow runoff components to precipitation change in the continental United States, *Water Resour. Res.*, 47, W02523, doi:10.1029/2010WR009656, 2011.
- Horton, R. E.: Drainage basin characteristics, *Eos Trans.*, 13, 350–361, 1932.
- Horton, R. E.: Erosional development of streams and their drainage basins: hydro-physical approach to quantitative morphology, *Geol. Soc. Am. Bull.*, 56, 275–370, 1945.
- Hunrichs, R. A.: Identification and classification of perennial streams of Arkansas, US Geological Survey, Water Resources Investigations Report 83-4063, 1983.
- Ivkovic, K. M.: A top-down approach to characterise aquifer-river interaction processes, *J. Hydrol.*, 365, 145–155, 2009.
- Johnston, C. A. and Shmagin, B. A.: Regionalization, seasonality, and trends of streamflow in the US Great Lakes Basin, *J. Hydrol.*, 362, 69–88, 2008.
- Kelson, K. I. and Wells, S. G.: Geologic influences on fluvial hydrology and bedload transport in small mountainous watersheds, northern New Mexico, USA, *Earth Surf. Proc. Land.*, 14, 671–690, 1989.
- Lyne, V. and Hollick, M.: Stochastic time-variable rainfall-runoff modeling, In: *Proc. Hydrology and Water Resources Symposium*, Perth, 89–92, Inst. Of Engrs, Australia, 1979.
- Madduma Bandara, C. M.: Drainage density and effective precipitation, *J. Hydrol.*, 21, 187–190, 1974.
- McIntosh, B. A., Sedell, J. R., Thurow, R. F., Clarke, S. E., and Chandler, G. L.: Historical changes in pool habitats in the Columbia River Basin, Report to the Eastside Ecosystem Management Project, Walla Walla, WA, 1995.
- Meinzer, O. E.: Outline of ground-water hydrology, with definitions, Washington, DC, US Geological Survey, Water Supply Paper 494, 1923.
- Melton, M. A.: An analysis of the relations among elements of climate, surface properties, and geomorphology, Tech. Rep. 11, Off. Nav. Res. Proj. 389-042, Dep. of Geol., Columbia Univ., New York, 1957.
- Merz, R. and Blöschl, G.: Flood frequency hydrology: 1. Temporal, spatial, and causal expansion of information, *Water Resour. Res.*, 44, W08432, doi:10.1029/2007WR006744, 2008.
- Milly, P. C. D.: Climate, soil water storage, and the average annual water balance, *Water Resour. Res.*, 30, 2143–2156, 1994.
- Moglen, G. E., Eltahir, E. A. B., and Bras, R. L.: On the sensitivity of drainage density to climate change, *Water Resour. Res.*, 34, 855–862, 1998.
- Montgomery, D. R. and Dietrich, W. E.: Where do channels begin?, *Nature*, 336, 232–234, 1988.
- Pallard, B., Castellarin, A., and Montanari, A.: A look at the links between drainage density and flood statistics, *Hydrol. Earth Syst. Sci.*, 13, 1019–1029, doi:10.5194/hess-13-1019-2009, 2009.
- Perron, J. T., Mitrovica, J. X., Manga, M., Matsuyama, I., and Richards, M. A.: Evidence of an ancient martian ocean in the topography of deformed shorelines, *Nature*, 447, 840–843, 2007.
- Pike, J. G.: The estimation of annual runoff from meteorological data in a tropical climate, *J. Hydrol.*, 2, 116–123, 1964.
- Sankarasubramanian, A. and Vogel, R. M.: Annual hydroclimatology of the United States, *Water Resour. Res.*, 38, 1083, doi:10.1029/2001WR000619, 2002a.
- Sankarasubramanian, A. and Vogel, R. M.: Comment on: “Basin hydrologic response relations to distributed physiographic descriptors and climate”, *J. Hydrol.*, 263, 257–261, 2002b.
- Simley, J.: National Hydrography Dataset Newsletter, US Geological Survey Report, Vol. 2, 2003.
- Simley, J.: National Hydrography Dataset Newsletter, US Geological Survey Report, Vol. 5, 2006.
- Simley, J.: National Hydrography Dataset Newsletter, US Geological Survey Report, Vol. 6, 2007.
- Sivapalan, M.: Pattern, processes and function: elements of a unified theory of hydrology at the watershed scale, in: *Encyclopedia of hydrological sciences*, edited by: Anderson, M., London, John Wiley, 193–219, 2005.
- Sivapalan, M., Yaeger, M. A., Harman, C. J., Xu, X., and Troch, P. A.: Functional model of water balance variability at the catchment scale: 1. Evidence of hydrologic similarity and space-time symmetry, *Water Resour. Res.*, 47, W02522, doi:10.1029/2010WR009568, 2011.
- Thornthwaite, C.: The climates of North America according to a new classification, *Geogr. Rev.*, 21, 633–655, 1931.
- Turc, L.: Le bilan d'eau des sols: Relation entre les précipitations, l'évaporation et l'écoulement, *Ann. Agron.*, 5, 491–569, 1954.
- Van Beek, L. P. H. and Bierkens, M. F. P.: The global hydrological model PCR-Globwb: conceptualization, parameterization and verification, Report Department of Physical Geography, Utrecht University, Utrecht, The Netherlands, available at: <http://vanbeek.geo.uu.nl/suppinfo/vanbeekbierkens2009.pdf> (last access: 23 January 2013), 2008.
- Wagener, T., Sivapalan, M., Troch, P., and Woods, R.: Watershed classification and hydrologic similarity, *Geography Compass*, 1, 901, doi:10.1111/j.1749-8198.2007.00039.x, 2007.

- Wang, D. and Alimohammadi, N.: Responses of annual runoff, evaporation and storage change to climate variability at the watershed scale, *Water Resour. Res.*, 48, W05546, doi:10.1029/2011WR011444, 2012.
- Wang, D. and Hejazi, M.: Quantifying the relative contribution of the climate and direct human impacts on mean annual streamflow in the contiguous United States, *Water Resour. Res.*, 47, W00J12, doi:10.1029/2010WR010283, 2011.
- Wigington, P. J., Moser, T. J., and Lindeman, D. R.: Stream network expansion: a riparian water quality factor, *Hydrol. Process.*, 19, 1715–1721, 2005.
- Wu, H., Kimball, J. S., Mantua, N., and Stanford, J.: Automated up-scaling of river networks for macroscale hydrological modeling, *Water Resour. Res.*, 47, W03517, doi:10.1029/2009WR008871, 2011.
- Yang, D., Sun, F., Liu, Z., Cong, Z., Ni, G., and Lei, Z.: Analyzing spatial and temporal variability of annual water-energy balance in nonhumid regions of China using the Budyko hypothesis, *Water Resour. Res.*, 43, W04426, doi:10.1029/2006WR005224, 2007.
- Yang, H., Yang, D., Lei, Z., and Sun, F.: New analytical derivation of the mean annual water-energy balance equation, *Water Resour. Res.*, 44, W03410, doi:10.1029/2007WR006135, 2008.
- Yokoo, Y., Sivapalan, M., and Oki, T.: Investigating the roles of climate seasonality and landscape characteristics on mean annual and monthly water balances, *J. Hydrol.*, 357, 255–269, 2008.
- Zhang, L., Potter, N., Hickel, K., Zhang, Y., and Shao, Q.: Water balance modeling over variable time scales based on the Budyko framework – Model development and testing, *J. Hydrol.*, 360, 117–131, 2008.
- Zhang, L., Dawes, W. R., and Walker, G. R.: Response of mean annual evapotranspiration to vegetation changes at watershed scale, *Water Resour. Res.*, 37, 701–708, 2001.